pyrophosphate, $(VO)_2P_2O_7 \cdot 2H_2O$.[29]

The topotactic nature of the transformation from $VO(HPO_4) \cdot 0.5H_2O$ to $(VO)_2P_2O_7$, the active catalyst for the oxidation of butane to maleic anhydride, explains the crucial role of precursor morphology in determining catalyst performance which has been previously noted.[26] By synthesizing $VO(HPO_4) \cdot 0.5H_2O$ in alcoholic solvents under certain conditions,[26a] crystals with a plate-like morphology having the (001) face exposed are formed. The topotactic dehydration results in $(VO)_2P_2O_7$ with the (020) face of the resulting platelike crystallites being the major crystal face exposed.

Experimental Section

Unless otherwise noted, all procedures were carried out in air. Reagent grade V_2O_5, 85% H_3PO_4, and 95% EtOH were used as received. $VOPO_4 \cdot 2H_2O$ was prepared as described previously.[10,35] 2-Butanol (Aldrich, 99%) showed no 2-butanone by GLC analyses. Vanadium oxidation state measurements were performed by redox titrimetry, oxidizing the sample with a known excess of Ce^{4+}, and titrating the mixture with Fe^{2+} to determine unreacted Ce^{4+} and total V^{5+}. Powder X-ray diffraction patterns were measured on a Siemens D-500 automated diffractometer using monochromated Cu Kα radiation, with a 0.02° 2θ step every 5 s for an effective scan rate of 0.24° 2θ/min. An automatic routine subtracted Cu Kα_2 peaks and provided integrated intensities. Elemental analyses were performed by Galbraith Laboratories. FT-IR spectra, run in KBr pellets, and scanning electron micrographs were obtained from the ER&E Analytical and Information Division. Thermogravimetric analyses were done using either a Du Pont thermal analyzer, Models 951 and 990, or an evacuable Fisher 260F microbalance at a heating rate of 10 °C/min. GLC was done with a Hewlett-Packard 5840A with a Carbowax (10 ft., 10% on Chromasorb WHP) column at 90 °C and quantified by the standard addition method. Paper chromatography was performed as described in the literature.[47] Samples were dissolved in 0.02 M Na_4EDTA, as were standards of NaH_2PO_4 and $Na_4P_2O_7$. Orthophosphate gave an R_f value of 0.76, pyrophosphate gave 0.50. Only orthophosphate was observed in $VO(HPO_4) \cdot 0.5H_2O$. Magnetization measurements were carried out by using a modified George Associates Faraday Magnetometer equipped with a Perkin-Elmer AR-2 vacuum microbalance and a 4-in. Varian Electromagnet and constant current supply. The sample used for magnetic measurements was synthesized from highest purity commercially available starting materials. The accuracies of the reported temperatures and susceptibilities are ~1 K and ~1%, respectively.

Reaction of $VOPO_4 \cdot 2H_2O$ with 2-Butanol. $VOPO_4 \cdot 2H_2O$ (8.00 g, 0.0404 mol) was refluxed with stirring in 2-butanol (160 mL) for 21 h. After cooling, the resulting solid was filtered. 2-Butanone (0.010 g, 0.126 mol) was detected in the yellow filtrate. The solid was washed four times with acetone (50 mL). The initial washings were orange. The resulting light blue solid was dried in vacuo for 8 h to yield 4.74 g of $VO(HPO_4) \cdot 0.5H_2O$ (0.0276 mol, 68.2%). Anal. [Found (Calcd)]: 28.59% V (29.63), 18.19% P (18.02), 1.23% H (1.17).

Reaction of V_2O_5 with H_3PO_4 in Ethanol. V_2O_5 (15.00 g, 0.0825 mol) was refluxed with stirring in 95% EtOH (900 mL) containing H_3PO_4 (22.6 mL, 0.330 mol). During the reaction the suspension changed from orange to olive-green to pale blue-green. After 11 days, the solid was filtered from the clear supernatant, washed with acetone, and dried in vacuo for 16 h to yield 28.46 g of $VO(HPO_4) \cdot 0.5H_2O$ (0.166 mol, 100%). Anal. [Found (Calcd)]: 29.39% V (29.63), 17.79% P (18.02), 1.31% H (1.17).

Preparation of Deuterated Analogue. The reaction was set up in a flowing N_2 drybox to prevent H/D exchange with atmospheric moisture. The V_2O_5 and the glassware were oven-dried at 150 °C before use. V_2O_5 (0.300 g, 1.65 mmol) was placed in a 25-mL flask with ethanol-d_6 (99% D, 9.00 g), D_2O (0.50 g), and D_3PO_4 (85% in D_2O, 0.79 g, 6.65 mmol). The flask was fitted with a stirring bar and reflux condenser topped by a $CaSO_4$-filled drying tube and removed from the drybox. The mixture was refluxed with stirring for 11 days, cooled, and filtered. The resulting blue solid was washed with D_2O and dried at 60 °C in vacuo for 16 h to yield 0.567 g of $VO(DPO_4) \cdot 0.5D_2O$ (3.26 mmol, 98.8%).

Thermal Reactions of $VO(HPO_4) \cdot 0.5H_2O$. $VO(HPO_4) \cdot 0.5H_2O$ was placed in an alumina boat inside a silica tube in an electric furnace. Helium was passed through the tube while heating. The temperature inside the tube was monitored with a thermocouple placed immediately over the sample. The tube was purged overnight with helium before heating began. Samples were weighed before and after reaction on an analytical balance.

Acknowledgment. We thank H. J. Brady and J. A. Panella for TGA and M. E. Leonowicz for assistance in indexing the powder X-ray pattern of $VO(HPO_4) \cdot 0.5H_2O$. K. K. Rao, T. C. Yang, E. N. Suciu, and others of Exxon Chemical Company participated in helpful discussions concerning $VO(HPO_4) \cdot 0.5H_2O$ and its relation to maleic anhydride catalysts.

Note Added in Proof. The crystal structure of $VO(HPO_4) \cdot 0.5H_2O$ has recently been described.[48]

Registry No. $VOPO_4 \cdot 2H_2O$, 12359-27-2; $VO(HPO_4) \cdot 0.5H_2O$, 93280-40-1; $(VO)_2P_2O_7$, 58834-75-6; V_2O_5, 1314-62-1; 2-butanol, 78-92-2.

(47) Bernhard, D. N.; Chess, W. B. *Anal. Chem.* **1959**, *31*, 1026-1029.

(48) Torardi, C. C.; Calabrese, J. C. *Inorg. Chem.* **1984**, *23*, 1308-1310.

Dinuclear Elimination from Rhenium Hydrides and $AlMe_3$: Rhenium/Aluminum Polyhydrides

Wincenty A. Skupiński, John C. Huffman, Joseph W. Bruno, and Kenneth G. Caulton*

Contribution from the Department of Chemistry and Molecular Structure Center, Indiana University, Bloomington, Indiana 47405. *Received March 26, 1984*

Abstract: Reaction of Al_2Me_6 with ReH_7P_2 and with ReH_5P_3 (P = PMe_2Ph and $PMePh_2$) in benzene occurs with methane elimination to give $ReH_6AlMe_2P_2$ and $ReH_4AlMe_2P_3$, respectively. Each bimetallic compound is fluxional and shows evidence for both bridging and terminal hydride ligands. The X-ray crystal structure of $ReH_6AlMe_2(PMePh_2)_2$ shows it to be based on a ReH_6P_2 dodecahedron with $AlMe_2$ bound to two hydride ligands, forming a η^2-H_2AlMe_2 unit. Crystallographic data (−162 °C): triclinic, $P\bar{1}$ with $Z = 2$ and $a = 17.815$ (8) Å, $b = 10.386$ (4) Å, $c = 11.094$ (4) Å, $\alpha = 111.47$ (2)°, $\beta = 86.08$ (2)°, $\gamma = 95.78$ (2)°. The X-ray crystal structure of $ReH_4AlMe_2(PMePh_2)_3$ shows a ReH_4P_3 pentagonal bipyramid (one P axial and two equatorial) with $AlMe_2$ attached through *three* hydride ligands, one axial and two equatorial on Re, forming a $H_3AlMe_2^{2-}$ unit. Crystallographic data (−164 °C): monoclinic, $P2_1/a$ with $Z = 4$ and $a = 15.053$ (4) Å, $b = 15.900$ (4) Å, $c = 11.705$ (2) Å, and $\beta = 92.59$ (1)°. Evidence for the mechanism of these reactions is presented, and the trend for aluminum to achieve a coordination number greater than 4 is surveyed.

An open coordination site (i.e., a 16-valence electron configuration) is thought to be a prerequisite for binding a donor substrate to a metal complex. This being the case, we speculated that covalent attachment of an aluminum Lewis acid to a transition metal (eq 1) might provide a bimetallic complex with unsaturation at the main-group center which could provide a new means for

0002-7863/84/1506-8128$01.50/0

$$L_nMX + YAlR_2 \longrightarrow L_nM\text{-}AlR_2 + X\text{-}Y \quad (1)$$

substrate activation. A model for such a compound is monomeric $Cp(OC)_3W$–$GaMe_2$,[1] which contains trigonal-planar gallium. Since our goal was subsequent reduction of the desired aluminum-bound substrate, we desired that the ligand complement of M include hydride ligands. A polyhydride complex was therefore selected for the coupling reaction with aluminum. We report here the characterization of the bimetallic compounds which were realized by this procedure and discuss the nature of the aluminum hydride interactions in these.

Experimental Section

All operations were performed under N_2 for exclusion of oxygen and moisture, using either Schlenk or, preferably, glovebox techniques. Solvents were dried with liquid Na/K alloy. NMR spectra were recorded in sealed tubes on Varian T-60, HR-220, and Nicolet 360 spectrometers. Phosphorus chemical shifts are relative to external 85% H_3PO_4, with downfield shifts being positive. All J values are given in hertz.

Synthetic Work. $ReCl_3(PPh_2Me)_3$.[2] Perrhenic acid (as an acidic aqueous solution containing 0.52 g of Re) and 1.7 mL of concentrated HCl were added to 20 mL of ethanol. A total of 2 mL (2.2 g) of PPh_2Me was added and the mixture was refluxed 15 min to yield a yellow precipitate. The solution was cooled to 25 °C, filtered, and the solid washed with 2 × 5 mL of ethanol to give 1.6 g (90%) of $ReCl_3(PPh_2Me)_3$.

$ReH_5(PPh_2Me)_3$. To $ReCl_3(PPh_2Me)_3$ (1.6 g) in 30 mL of ethanol was added 0.8 g of $NaBH_4$. The mixture was heated to reflux, resulting in H_2 evolution and a color change from yellow to pale orange. Whe H_2 evolution ceased, the solution was cooled to 25 °C and the solvent removed under vacuum. The hydride product was extracted from the solid residue with 3 × 20 mL of benzene. The benzene was removed in vacuum and the solid residue recrystallized from 20 mL of hot ethanol by cooling to −10 °C: yield, 0.9 g (90%); IR (Nujol) 1983 (sh), 1959 (sh), 1940 (m), 1893 (sh), 1880 (m) cm^{-1}; NMR (C_6D_6) δ $^{31}P\{^1H\}$ 6.2 (s); ^1H δ P–Ph, and 1.90 (PMe), −5.50 (q, J = 23, ReH).

$ReCl_4(PPh_2Me)_2$.[2] Chlorine was bubbled through $ReCl_3(PPh_2Me)_3$ (1.5 g) suspended in CCl_4 for 15 min. The resulting dark red precipitate of $ReCl_4(PPh_2Me)_2$ was filtered, washed with CCl_4, and dried in vacuum. The yield is quantitative.

$ReH_7(PPh_2Me)_2$. $NaBH_4$ (1.0 g) was added to a suspension of 1.5 g of $ReCl_4(PPh_2Me)_2$ in 95 mL of ethanol. The temperature during this addition was limited to 10–20 °C with an ice bath to minimize conversion of $ReH_7(PPh_2Me)_2$ to a red product. The reaction was marked by hydrogen evolution and a color change from violet to pale yellow. Hydrogen evolution is essentially complete after 2.5 h. The solvent was then removed in vacuum, the residue extracted with 20 mL of benzene, and the resulting red solution evaporated to dryness in vacuum. The solid residue was dissolved in 15 mL of THF, 30 mL of EtOH was added, and the solution concentrated under vacuum (no heating!). The resulting material (a mixture of red and white solids) was filtered, dissolved in a minimum of THF, and diluted (in air) with 5 volumes of ethanol. After 12 h in a refrigerator, white and green solids have precipitated. These solids were filtered and washed with methanol, which selectively dissolves away the green solid: yield, 40%. **Note**: All operations must be carried out below 30 °C. IR (Nujol): 2000 (sh), 1990 (sh), 1970 (sh), 1900 (m) cm^{-1}. ^1H NMR (in toluene at 60 MHz and 25 °C): unresolved aromatic resonances and 2.30 (PMe) and −4.72 (t, J = 20, Re–H).

$ReH_4AlMe_2(PPh_2Me)_3$. All operations are best carried out in a glovebox. $ReH_5(PPh_2Me)_3$ (0.12 g, 0.15 mmol) was dissolved in a minimum of benzene and 0.2 mL of a 1 M $AlMe_3$ solution (0.2 mmol Al) was added. The resulting solution is heated under N_2 in an 80–95 °C oil bath for 6 h. Nearly all of the benzene was then removed under vacuum and hexane was added to the resulting concentrated but homogeneous benzene solution. Cooling overnight in a refrigerator yielded pale yellow needle crystals. These were filtered, washed with hexane, and dried under vacuum. Crystals for X-ray diffraction were obtained by recrystallization from hot (60 °C) toluene/hexane, by slow cooling of the heating bath and recrystallization tube to 25 °C. The synthetic reaction also proceeds in toluene solvent or as a suspension in hexane: IR (Nujol) 1965 (m), 1890 (m), 1803 (sh), 1765 (m), 1680 (s) cm^{-1}; ^1H NMR (at 16 °C in toluene-d_8, δ scale) 7.24 (t, o-phenyl, 12 H), 6.94 (m, m- + p-phenyl), 18 H), 1.68 (d, J = 7 Hz, 9 H), −0.18 (s, MeAl, 6 H), −7.76 (q, J = 18 Hz, hydride, 4 H); at 360 MHz and −70 °C in toluene-d_8 7.48 (s), 6.85 (s), 1.38 (s), −0.02 (s, AlMe), −0.04 (s, AlMe), −6.3 (br s, 1 H, Re–H), −8.3 (br s, 3 H, Re···H···Al); $^{31}P\{^1H\}$ NMR (toluene-d_8) δ +5.6 (s) at +30 °C, +8.8 (br s, $\Delta\nu_{1/2}$ = 110 Hz) at −80 °C; selectively hydride-coupled ^{31}P NMR δ +5.6 (quintet, J = 15 Hz).

$ReH_6AlMe_2(PPh_2Me)_2$. All operations are best carried out in a glovebox. $ReH_7(PPh_2Me)_2$ (0.06 g, 0.1 mmol) in 1 mL of benzene and 0.1 mL of 1 M benzene solution of $AlMe_3$ (0.1 mmol of Al) were combined. Gas evolution was vigorous; the reaction was complete in 15 min at 25 °C. The resulting yellow solution was concentrated almost to the cloud point and hexane added. Storage overnight at −20 °C produced a white solid. Recrystallization from hexane (by heating to 60 °C, followed by slow cooling to 25 °C) yielded colorless crystals suitable for X-ray crystallography: IR (Nujol) 2005 (w), 1970 (m), 1930 (m), 1780 (m), 1758 (s) cm^{-1}; ^1H NMR (60 MHz in toluene at 25 °C) unresolved aromatic resonances and 2.06 (PMe) and −6.08 (t, J = 15 Hz, hydride); $^{31}P\{^1H\}$ NMR (40.5 MHz in C_6D_6 at 30 °C) +4.3 ppm (s).

Analogous reaction of $ReH_5(PMe_2Ph)_3$ and $ReH_7(PMe_2Ph)_2$ with $AlMe_3$ gave products with the following spectral parameters.

$ReH_4AlMe_2(PMe_2Ph)_3$: ^1H NMR (360 MHz in C_6D_6 at 25 °C) 7.48 (t, o-phenyl), 7.08 (m, m- + p-phenyl), 1.51 (d, J = 7 Hz, PMe), 0.06 (s, AlMe), −8.24 (q, J = 17 Hz, hydride). The hydride resonance of $ReH_5(PMe_2Ph)_3$ is at δ −6.08 (J = 18.7 Hz).

$ReH_6AlMe_2(PMe_2Ph)_2$: ^1H NMR (60 MHz in C_6H_6 at 25 °C) unresolved aromatic resonances and δ 1.60 (d, J = 8, PMe, 12 H), 0.27 (s, AlMe), −6.47 (t, J = 16, hydride, 6 H). The hydride resonance of $ReH_7(PMe_2Ph)_2$ is at δ −5.18 (J = 20 Hz).

All rhenium aluminum compounds reported here react rapidly with water to reform the corresponding parent hydride, ReH_7P_2 or ReH_5P_3.

X-ray Crystallography. $ReH_6AlMe_2(PPh_2Me)_2$. A suitable crystal was transferred to the goniostat using standard inert-atmosphere handling techniques.[3] A systematic search of a limited hemisphere of reciprocal space revealed a monoclinic lattice which could be indexed as $P2_1/a$ (alternate setting of $P2_1/c$). Parameters of the data collected ($6° \leq 2\theta \leq 50°$) appear in Table I. The structure was solved by Patterson techniques and direct methods in combination with Fourier techniques. All hydrogen atoms were located and refined isotropically, with nonhydrogens assigned anisotroic thermal parameters. A final difference Fourier was featureless, the largest peak being 0.4 e/Å^3.

Results of the structure study appear in Tables II and III and Figures 1 and 2. Anisotropic thermal parameters, observed and calculated structure factors, and hydrogen positional parameters are available as supplementary material.

Table I. Crystal Data for $ReH_4AlMe_2(PMePh_2)_3$ and $ReH_6AlMe_2(PMePh_2)_2$

formula	$C_{28}H_{38}AlP_2Re$	$C_{41}H_{49}AlP_3Re$
color of crystal	pale yellow	pale yellow
crystal dimensions, mm	0.06 × 0.09 × 0.10	0.24 × 0.28 × 0.28
space group	$P2_1/a$	$P\bar{1}$
cell dimensions	−164 °C, 40 reflections	−162 °C, 46 reflections
a, Å	15.053 (4)	17.815 (8)
b, Å	15.900 (4)	10.386 (4)
c, Å	11.705 (2)	11.094 (4)
α, deg		111.47 (2)
β, deg	92.59 (1)	86.08 (2)
γ, deg		95.78 (2)
molecules/cell	4	2
volume, Å^3	2798.63	1899.49
calcd density, gm/cm^3	1.54	1.48
wavelength, Å	0.710 69	0.710 69
mol wt	649.74	847.94
linear absorption coeff, cm^{-1}	45.58	34.16
no. of unique intensities collected	4935	4966
no. with $F > 0.0$	4540	4855
no. with $F > \sigma(F)$	4324	4765
no. with $F > 2.33\sigma(F)$	4014	4627
final residuals		
$R(F)$	0.0454	0.0204
$R_w(F)$	0.0398	0.0216
goodness of fit for the last cycle	1.36	0.72
max Δ/σ for last cycle	0.05	0.05

(1) St. Denis, J. N.; Butler, W.; Glick, M. D.; Oliver, J. P. *J. Organomet. Chem.* **1977**, *129*, 1.

(2) Chatt, J.; Leigh, G. J.; Mingos, D. M. P.; Paske, R. J. *J. Chem. Soc. A* **1968**, 2636.

(3) Huffman, J. C.; Lewis, L. N.; Caulton, K. G. *Inorg. Chem.* **1980**, *19*, 2755.

Table II. Fractional Coordinates[a] and Isotropic Thermal Parameters for $ReH_6AlMe_2(PMePh_2)_2$

	10^4x	10^4y	10^4z	$10B_{iso}$[b]
Re(1)	8864.4 (2)	4902.9 (2)	7583.8 (2)	12
Al(2)	8625 (2)	3344 (1)	7469 (2)	16
C(3)	7793 (6)	2818 (6)	6356 (8)	27
C(4)	9224 (6)	2515 (5)	8455 (7)	21
P(5)	7759 (1)	5981 (1)	7603 (2)	13
C(6)	7478 (6)	6444 (6)	6208 (8)	19
C(7)	7958 (5)	6912 (5)	8523 (6)	16
C(8)	8166 (5)	6795 (5)	9672 (7)	17
C(9)	8267 (5)	7486 (6)	10412 (8)	23
C(10)	8158 (6)	8292 (5)	9972 (8)	25
C(11)	7961 (6)	8406 (5)	8838 (8)	24
C(12)	7872 (5)	7726 (5)	8097 (8)	20
C(13)	6649 (5)	5644 (4)	8016 (6)	13
C(14)	6150 (5)	6098 (5)	8781 (7)	20
C(15)	5288 (6)	5840 (6)	9006 (8)	24
C(16)	4918 (5)	5148 (6)	8471 (7)	24
C(17)	5407 (6)	4693 (5)	7720 (8)	25
C(18)	6270 (5)	4929 (5)	7492 (7)	22
P(19)	10114 (1)	5821 (1)	7462 (2)	14
C(20)	10466 (6)	6321 (5)	8801 (7)	21
C(21)	9959 (5)	6704 (4)	6457 (7)	16
C(22)	9966 (6)	7533 (5)	6841 (7)	22
C(23)	9803 (7)	8178 (6)	6072 (9)	32
C(24)	9634 (6)	8020 (5)	4925 (8)	25
C(25)	9622 (6)	7197 (6)	4537 (8)	25
C(26)	9795 (5)	6549 (5)	5301 (7)	19
C(27)	11180 (5)	5353 (4)	7064 (7)	15
C(28)	11717 (5)	5709 (5)	6280 (7)	18
C(29)	12546 (6)	5372 (6)	6079 (7)	22
C(30)	12844 (5)	4675 (5)	6697 (7)	20
C(31)	12305 (5)	4319 (5)	7484 (7)	19
C(32)	11479 (5)	4641 (5)	7655 (7)	19
H(1)	888 (6)	522 (5)	654 (8)	22 (19)
H(2)	880 (4)	535 (4)	878 (5)	0 (12)
H(3)	945 (5)	449 (5)	853 (7)	15 (16)
H(4)	809 (6)	451 (5)	668 (7)	25 (19)
H(5)	921 (5)	413 (5)	670 (7)	18 (17)
H(6)	818 (8)	434 (7)	834 (10)	58 (30)

[a] Fractional coordinates are times 10^3 for metal-bound hydrogens. [b] Isotropic values for those atoms refined anisotropically are calculated using the formula give by Hamilton, W. C. *Acta Crystallogr.* **1959**, *12*, 609.

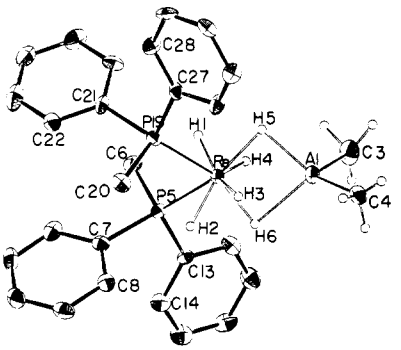

Figure 1. Atom labeling on $ReH_6AlMe_2(PPh_2Me)_2$. Phosphine hydrogens have been deleted for clarity.

$ReH_4AlMe_2(PPh_2Me)_3$. A well-formed crystal was transferred to the goniostat using standard inert-atmosphere handling techniques.[3] The crystal appeared to be somewhat thermochromic, becoming colorless upon cooling to −162 °C. A systematic search of a limited hemisphere of reciprocal space revealed no systematic absences or symmetry, indicating a triclinic space group. Subsequent solution and refinement of data ($6° \leq 2\theta \leq 45°$) collected at −162 °C confirmed this choice. Parameters of the data collected appear in Table I. The structure was solved by direct methods (MULTAN78) and Fourier syntheses. All hydrogen atoms were located in a difference Fourier synthesis phased on the non-hydrogen atoms. Final full-matrix refinement included all positional parameters, isotropic thermal parameters for hydrogens, anisotropic thermal parameters for non-hydrogen atoms, an overall scale factor, and a secondary extinction parameter. A final difference Fourier synthesis was featureless, the largest peak being 0.45 e/Å^3.

Results of the structure study are shown in Tables IV and V and Figures 5 and 6. Refined C–H distances range from 0.81 (5) to 1.02 (6) Å; for any single chemical type, the range of values is always less than 3σ. Anisotropic thermal parameters, observed and calculated structure factors, and hydrogen positional parameters are available as supplementary material.

Table III. Selected Bond Distances (Å) and Angles (deg) for $ReH_6AlMe_2(PMePh_2)_2$

Re–P(5)	2.391 (2)
Re–P(19)	2.390 (2)
Re–Al	2.508 (2)
Re–H(1)	1.33 (9)
Re–H(2)	1.57 (6)
Re–H(3)	1.53 (8)
Re–H(4)	1.66 (9)
Re–H(5)	1.70 (8)
Re–H(6)	1.65 (12)
Al–H(5)	1.79 (8)
Al–H(6)	2.02 (12)
P(5)–C(6)	1.823 (9)
P(5)–C(7)	1.846 (8)
P(5)–C(13)	1.840 (7)
P(19)–C(20)	1.815 (9)
P(19)–C(21)	1.841 (7)
P(19)–C(27)	1.847 (7)
Al–C(3)	1.954 (9)
Al–C(4)	1.946 (9)
P(5)–Re–P(19)	96.5 (1)
P(5)–Re–Al	127.7 (1)
P(19)–Re–Al	135.4 (1)
Re–Al(2)–C(3)	123.0 (3)
Re–Al(2)–C(4)	125.2 (3)
C(3)–Al(2)–C(4)	111.8 (4)
P(5)–Re–H(1)	77 (4)
P(5)–Re–H(2)	66 (2)
P(5)–Re–H(3)	133 (3)
P(5)–Re–H(4)	79 (3)
P(5)–Re–H(5)	139 (3)
P(5)–Re–H(6)	86 (4)
P(19)–Re–H(1)	71 (4)
P(19)–Re–H(2)	82 (2)
P(19)–Re–H(3)	83 (3)
P(19)–Re–H(4)	136 (3)
P(19)–Re–H(5)	98 (3)
P(19)–Re–H(6)	151 (4)
Al–Re–H(1)	109 (4)
Al–Re–H(2)	118 (2)
Al–Re–H(3)	72 (3)
Al–Re–H(4)	60 (3)
Al–Re–H(5)	46 (3)
Al–Re–H(6)	53 (4)
H(1)–Re–H(2)	131 (4)
H(1)–Re–H(3)	143 (5)
H(1)–Re–H(4)	66 (5)
H(1)–Re–H(5)	72 (5)
H(1)–Re–H(6)	137 (6)
H(2)–Re–H(3)	67 (4)
H(2)–Re–H(4)	132 (4)
H(2)–Re–H(5)	154 (4)
H(2)–Re–H(6)	73 (5)
H(3)–Re–H(4)	132 (4)
H(3)–Re–H(5)	87 (4)
H(3)–Re–H(6)	74 (5)
H(4)–Re–H(5)	64 (4)
H(4)–Re–H(6)	73 (5)
H(5)–Re–H(6)	99 (5)
H(5)–Al(2)–H(6)	83 (4)
Re–H(5)–Al	92 (4)
Re–H(6)–Al	86 (5)

Results

Dinuclear Elimination with Rhenium Heptahydrides. The d^0 complexes ReH_7P_2 (P = PMe_2Ph and PPh_2Me) react rapidly at 25 °C with equimolar (1:1 Re:Al) Al_2Me_6 to produce $ReH_6AlMe_2P_2$ and methane. The complex with PMe_2Ph, because

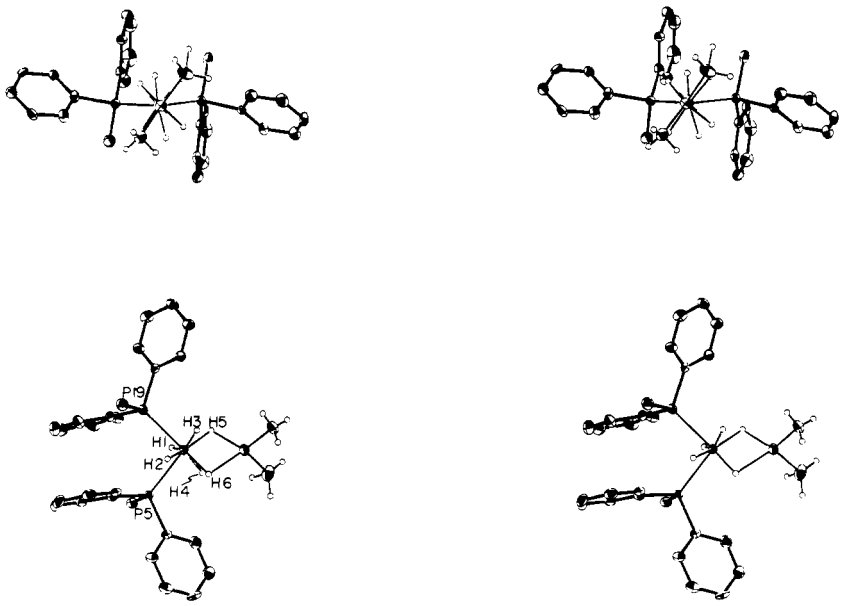

Figure 2. Stereoviews of $ReH_6AlMe_2(PPh_2Me)_2$. Upper view is down the Re–Al vector and shows the fourfold staggered arrangement of ligands about rhenium. Lower view is perpendicular to the P5/P19/Re/Al plane and shows how the nonbridging H3 and H4 are more remote from aluminum than H5 and H6; this view is nearly down the intersection of the planes of the two trapezoids of the rhenium-centered dodecahedron. The trapezoids are defined by H6, H4, H1, P19, and H5, H3, H2, P5.

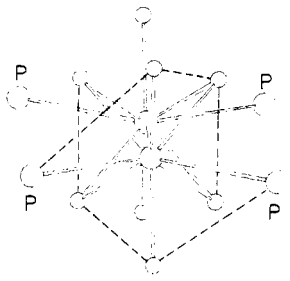

Figure 3. ORTEP drawing of the coordination spheres in $Re_2H_8(PEt_2Ph)_4$, using the atom coordinates of ref 3. Unlabeled terminal atoms are all hydrides. The sorting of ligands of the front rhenium into trapezoidal planes is shown with dashed lines.

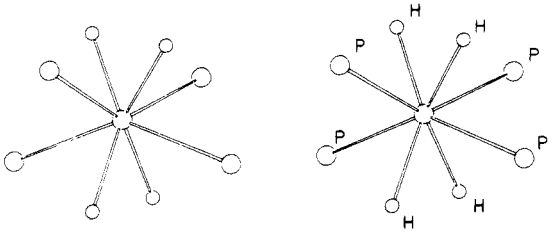

Figure 4. Stereo ORTEP drawing of the inner coordination sphere of $MoH_4(PMePh_2)_4$,[7] viewed down a C_2 axis of the dodecahedron. The S_4 axis is vertical in this view, and a second C_2 axis lies horizontally in the plane of the drawing.

of its high solubility in hexanes, was obtained only as an oil, but the PPh_2Me analogue could be obtained as a crystalline solid. The stoichiometry of these compounds was established from integration of the ^1H NMR spectrum at 25 °C. Retention of two phosphine ligands follows from the triplet structure of the hydride resonance, which itself suggests hydride fluxionality. The $^{31}P\{^1H\}$ NMR spectrum is a singlet at 30 °C. The compound shows three infrared-active terminal Re–H stretching vibrations (above 1900 cm^{-1}), along with two vibrations indicative of bridging hydrides (1780 and 1758 cm^{-1}).

The X-ray structure (Figures 1 and 2) of $ReH_6AlMe_2(PPh_2Me)_2$ reveals a nearly pianar ReP_2Al framework. The molecule closely approaches (noncrystallographic) C_2 symmetry, including methyl and phenyl groups (Figures 1 and 2), with aluminum lying on this C_2 axis. The presence of six metal-bound hydrogens is also revealed by the X-ray study. Two hydrogens,

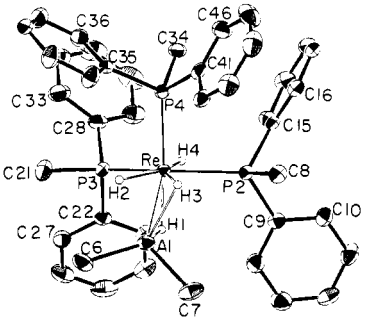

Figure 5. Atom labeling in $ReH_4AlMe_2(PPh_2Me)_3$, with all "organic" hydrogens deleted for clarity.

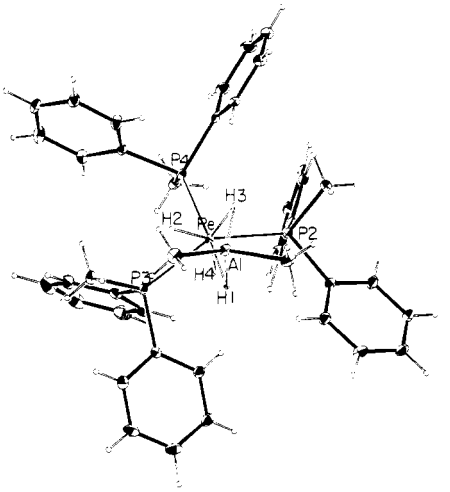

Figure 6. ORTEP drawing of $ReH_4AlMe_2(PPh_2Me)_3$ viewed nearly down the Re–Al vector.

H1 and H2, are unequivocally terminal on Re. The remaining four hydrogens are in the general Re–Al internuclear region (i.e., all bend toward aluminum). However, it is possible to sort these into a pair (H5 and H6) with shorter distances to Al and a pair (H3 and H4) with longer distances to Al. The latter pair also show a larger average angle Al–Re–H (66°) than the former (50°). This suggests the presence of an $H_2AlMe_2^-$ unit η^2 bound to Re. Independent confirmation comes from the fact that the

Table IV. Fractional Coordinates[a] and Isotropic Thermal Parameters for $ReH_4AlMe_2(PMePh_2)_3$

	10^4x	10^4y	10^4z	$10B_{iso}$[b]
Re(1)	3056.0 (1)	1088.6 (1)	3753.4 (1)	13
P(2)	2862 (1)	2450 (1)	5987 (1)	16
P(3)	2893 (1)	1366 (1)	1774 (1)	16
P(4)	1943 (1)	-364 (1)	3708 (1)	16
Al(5)	4435 (1)	763 (1)	3623 (1)	19
C(6)	4978 (2)	-322 (5)	2021 (4)	30
C(7)	5157 (2)	1657 (4)	5021 (5)	29
C(8)	3103 (2)	1710 (4)	7158 (4)	22
C(9)	3368 (2)	4180 (4)	6715 (4)	19
C(10)	3146 (2)	5046 (4)	7951 (4)	26
C(11)	3560 (3)	6276 (4)	8598 (4)	30
C(12)	4205 (2)	6662 (4)	8035 (4)	28
C(13)	4436 (2)	5830 (4)	6815 (4)	30
C(14)	4014 (2)	4597 (4)	6156 (4)	26
C(15)	1883 (2)	2876 (4)	6488 (3)	17
C(16)	1424 (2)	2242 (4)	7197 (4)	20
C(17)	676 (2)	2515 (4)	7476 (4)	25
C(18)	370 (2)	3441 (4)	7057 (4)	26
C(19)	829 (2)	4102 (4)	6364 (4)	28
C(20)	1575 (2)	3828 (4)	6086 (4)	23
C(21)	3181 (2)	-39 (4)	310 (4)	28
C(22)	3414 (2)	2930 (4)	1625 (4)	17
C(23)	3450 (2)	4178 (4)	2683 (4)	22
C(24)	3799 (2)	5368 (4)	2559 (4)	27
C(25)	4118 (2)	5352 (5)	1383 (5)	32
C(26)	4095 (2)	4130 (5)	329 (4)	31
C(27)	3750 (2)	2925 (4)	450 (4)	24
C(28)	1950 (2)	1617 (4)	1348 (4)	23
C(29)	1587 (2)	2745 (5)	2149 (4)	31
C(30)	864 (3)	2956 (5)	1849 (5)	39
C(31)	533 (3)	2026 (6)	757 (5)	44
C(32)	887 (3)	919 (6)	-40 (5)	45
C(33)	1593 (2)	710 (5)	245 (4)	32
C(34)	1031 (2)	354 (4)	3812 (4)	21
C(35)	1807 (2)	-1971 (4)	2259 (3)	17
C(36)	1280 (2)	-2144 (4)	1339 (4)	24
C(37)	1167 (2)	-3404 (5)	311 (4)	33
C(38)	1571 (2)	-4502 (4)	196 (4)	26
C(39)	2119 (3)	-4331 (4)	1071 (4)	29
C(40)	2231 (2)	-3072 (4)	2085 (4)	29
C(41)	1807 (2)	-1184 (4)	4958 (4)	20
C(42)	2429 (2)	-1667 (4)	5312 (4)	23
C(43)	2364 (3)	-2289 (4)	6233 (4)	31
C(44)	1668 (3)	-2426 (5)	6814 (4)	38
C(45)	1041 (3)	-1974 (5)	6467 (5)	39
C(46)	1114 (2)	-1360 (4)	5539 (4)	28
H(1)	388 (3)	210 (5)	369 (4)	41 (11)
H(2)	342 (4)	-7 (8)	265 (7)	105 (23)
H(3)	350 (2)	37 (4)	444 (4)	29 (9)
H(4)	259 (2)	237 (3)	394 (3)	6 (6)

[a] See Table II. [b] See Table II.

$AlMe_2$ plane is approximately perpendicular (98.2°) to that of Re–H5–H6.

The *pattern* of shorter Al–H distances (i.e., short to both H5 and H6, long to both H3 and H4) has symmetry which inspires confidence in our belief that H3 and H4 are nonbonding toward aluminum. Support for the idea that H3 (Al–H = 2.50 (8) Å) and H4 (Al–H = 2.22 (9) Å) do not bind to Al is found by comparison of these distances to a clearly nonbonding distance in this molecule: aluminum is 2.36 (23)–2.62 (14) Å from the hydrogens in the $AlMe_2$ group.

Further understanding of the atom connectivity in $ReH_6AlMe_2(PMePh_2)_2$ requires an assessment of the form of the eight-vertex ReH_6P_2 polyhedron. A view down the Re–Al line (Figure 2) of $ReH_6AlMe_2(PMePh_2)_2$ gives the visual impression of a fourfold staggered arrangement (H1, H2, P5, and P19 vs. H3, H4, H5, and H6). This is a feature which this compound shares with $H_2(PEt_2Ph)_2Re(\mu\text{-}H)_4ReH_2(PEt_2Ph)_4$,[4] Figure 3, and has led to that compound being idealized as square antiprismatic about each rhenium. Indeed, a view down the S_8 axis of a regular square antiprism (**1**) shows precisely this feature. The alternate

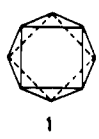

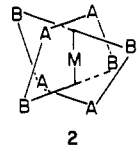

form of the eight-vertex polyhedron, the dodecahedron (**2**), has an S_4 axis which naturally sorts the vertices into two inequivalent types, A and B.[5] It is this natural accommodation of two different ligand types at different apices of two trapezoids in **2** which appears to be responsible for all structurally characterized $MH_4(PR_3)_4$[6a] and also $ReH_5(PMePh_2)_3$[6b] adopting idealized dodecahedral geometry. This preference is even stronger for such complexes since the B sites experience less interligand repulsion; they are invariably occupied by the bulky phosphine ligands.

In trying to establish the coordination polyhedron about rhenium in $ReH_6AlMe_2(PMePh_2)_2$, the key point is to recognize that a dodecahedron can also give the visual impression of two fourfold staggered arrays. This impression is gained by looking down either of the C_2 axes of rotation which lie perpendicular to the S_4 axis of **2**. This point of confusion is quite evident in Figure 4,[7] where $MoH_4(PMePh_2)_4$ is viewed down a C_2 axis of an authentic dodecahedron. Consequently, the best objective discrimination between structure **1** and **2** lies in (1) the presence or absence of two five-atom (metal plus four ligand) *planes* and (2) the mutual perpendicularity (or lack there of) of these planes. The relevant planes for $ReH_6AlMe_2(PMePh_2)_2$ are shown below, along with distances (Å) from the four-ligand least-squares planes.

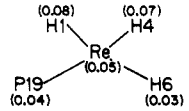

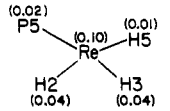

Also shown is the distance from rhenium to these planes. These data, and the angle between these two planes (88.3°), establish that the ReH_6P_2 coordination polyhedron approximates a dodecahedron in $ReH_6AlMe_2(PMePh_2)_2$. This conforms to the dodecahedral geometry found[6a] for $OsH_6(P\text{-}i\text{-}Pr_2Ph)_2$, another MH_6P_2 species.

The interligand angles within the two trapezoids of $ReH_6AlMe_2(PMePh_2)_2$ are displayed below.

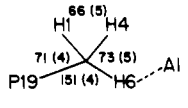

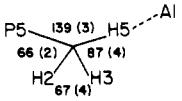

Angles related by the idealized C_2 symmetry are all equal to within 3σ and are quite consistent with neutron diffraction data on $ReH_5(PMePh_2)_3$.[6b]

The angle P–Re–P in $ReH_6AlMe_2(PMePh_2)_2$ is also diagnostic of coordination geometry. This angle, at 96.5 (1)° is much smaller than the angle between B sites within a single trapezoid in all MH_4P_4[6a] and $ReH_5(PMePh_2)_3$[6b] complexes (143–149°). It is also smaller than the angle (116 ± 4°) seen in numerous square antiprismatic MF_8^{n-} and $M(CN)_8^{n-}$ complexes.[8] This confirms the assignment (from the least-squares plane calculation) of the two phosphine ligands to different trapezoids in $ReH_6AlMe_2(PMePh_2)_2$. The P–Re–P angle is also much smaller than the P–Os–P angle (156.2°) seen for $OsH_6(P\text{-}i\text{-}Pr_2Ph)_2$,[6a] where both phosphines are in the same trapezoid. The P–Re–P angle is, however, similar to the angle (101°) found between orthogonal

(4) (a) Bau, R.; Carroll, W. E.; Hart, D. W.; Teller, R. G.; Koetzle, T. F. *Adv. Chem. Ser.* **1978**, *No. 167*, 73. (b) Bau, R.; Carroll, W. E.; Teller, R. G.; Koetzle, T. F. *J. Am. Chem. Soc.* **1977**, *99*, 3872.

(5) Hoard, J. L.; Silverton, I. V. *Inorg. Chem.* **1963**, *2*, 235.

(6) (a) Frost, P. W.; Howard, J. A. K.; Spencer, J. L. *Acta Crystallogr., Sect. C* **1984**, *40*, 946. (b) Emge, T. J.; Koetzle, T. F.; Bruno, J. W.; Caulton, K. G., submitted for publication in *Inorg. Chem.*

(7) Meakin, P.; Guggenberger, L. J.; Peet, W. G.; Muetterties, E. L.; Jesson, J. P. *J. Am. Chem. Soc.* **1973**, *95*, 1467.

(8) Kepert, D. L. *Prog. Inorg. Chem.* **1978**, *24*, 179.

trapezoid B-sites in $ReH_5(PMePh_2)_3$.[6b] The picture which emerges is that $ReH_6AlMe_2(PMePh_2)_2$ may be formally dissected into having $AlMe_2^+$ spanning two orthogonal trapezoid B-sites of dodecahedral $ReH_6P_2^-$, **3**. This structure does of course place

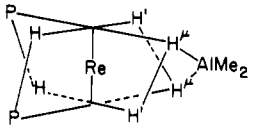

3

Al on an idealized C_2 axis of the dodecahedron, it uses the two most sterically unencumbered hydrides for bridging to Al, and it accounts for the two A-site hydrides (primed in **3**) bending toward aluminum, but to a much smaller extent than those which actually bridge. It is this attachment of aluminum to two B-sites in $ReH_6AlMe_2(PMePh_2)_2$, together with the tetrahedral geometry at Al, which dictates that the ReP_2 unit does not eclipse the $AlMe_2$ unit, but instead forms an angle close to 45° (observed at 52.3°).

The conclusion that $ReH_6AlMe_2(PMePh_2)_2$ adopts dodecahedral and not antiprismatic geometry at rhenium prompted us to reevaluate the geometry at rhenium in the structurally related $H_2(PEt_2Ph)_2Re(\mu\text{-}H)_4ReH_2(PEt_2Ph)_2$.[4] Since this dimer has four symmetrical hydride bridges, an assumed dodecahedral geometry at rhenium must distort from **3** so that the two H′ atoms become equivalent to the two H^μ in **3**. In fact, this model (Figure 3) naturally explains two features of the observed[4] structure of $Re_2H_8(PEt_2Ph)_4$ which are not accommodated by the square antiprismatic assumption:

(1) The P–Re–P angle (102.7 (2)°) is smaller than the H^μ–Re–H^μ angle (128.3 (4)°). These angles should be dictated by steric effects in an antiprism, and so the inequality should be reversed. However, the P–Re–P angle in a dodecahedron (Figure 3) is that between orthogonal-trapezoid B-sites, which we have noted above is tyically ~100°.

(2) The four μ-hydrides form a rectangle (not a square), whose shorter edge (1.87 Å compared to 2.04 Å) "crowds" (is directed toward) the bulky phosphines, not the smaller terminal hydrides. The opposite should be true in the square antiprism. In the dodecahedral model this closer approach of μ-hydrides derives from their "parentage" as cisoid A and B sites within one trapezoid. The longer nonbonded μ-H/μ-H distance follows naturally if it involves hydrides derived from different trapezoids.

The drawing below summarizes distances (Å) of atoms from the four-ligand least-squares planes shown in Figure 3, using neutron diffraction data, for $Re_2H_8(PEt_2Ph)_4$.[4]

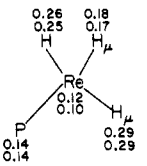

Two values are given since there are two crystallographically independent four-ligand sets; H_μ indicates hydrides which bridge to the other rhenium. The angle between these two planes is 86.5°. Taken together, all of the above evidence supports the idea that the ReH_6P_2 coordination geometry in $Re_2H_8(PEt_2Ph)_4$ may be represented as dodecahedral, distorted by the need to bring two B *and* two A sites into symmetrical bridging positions. Only in this latter aspect do the coordination geometries about rhenium differ in $Re_2H_8(PEt_2Ph)_4$ and $ReH_6AlMe_2(PMePh_2)_2$. For example, the trapezoids in $Re_2H_8(PEt_2Ph)_4$ have the following average internal angles (**4**), which may be compared in **5** to the

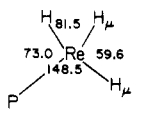

4

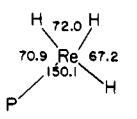

5

relevant neutron data for $ReH_5(PMePh_2)_3$.[6b] The major effect is clearly to draw one A-site hydrogen into bridging position, thus yielding a small H_μ–Re–H_μ angle.

Dinuclear Elimination with Rhenium Pentahydrides. At 25 °C, $ReH_5(PMe_2Ph)_3$ reacts only slowly with $AlMe_3$ in benzene (hours, with Al_2Me_6 in excess). At elevated temperatures and equimolar concentrations, the reaction proceeds smoothly with evolution of methane (by ^1H NMR) to give a product of empirical formula $ReH_xAlMe_2(PMe_2Ph)_3$; integration of the proton NMR spectrum gives $x = 4$. We lacked complete confidence in this method of determining x since alkyl aluminum hydrides themselves are notorious for showing no hydride resonance (^{27}Al had $I = {}^3/_2$). Moreover, this product, while pure by ^1H NMR, yielded only an oil after multiple attempts at crystallization. Effects were therefore turned to the PPh_2Me analogue of this complex. The dinuclear elimination synthesis (eq 2) proceeds equally well for this de-

$$^1/_2Al_2Me_6 + ReH_5(PPh_2Me)_3 \rightarrow ReH_xAlMe_2(PPh_2Me)_3 + \ldots \quad (2)$$

rivative, and crystalline solid is indeed obtainable. The value of x is best obtained from the selectively proton-decoupled ^{31}P NMR spectrum; when only the protons upfield of δ 0 are allowed to couple to P, a ^{31}P quintet is observed. The observation of a single phosphorus chemical shift, along with single resonances for P–Me, Re–H, and AlMe protons, all at 25 °C, suggests a fluxional molecule. The ^1H NMR at −70 °C and 360 MHz shows a 1:3 hydride pattern, two barely resolved Me(Al) groups, but still only one P–Me resonance (now broadened). At −80 °C and 40.5 MHz, the ^{31}P NMR spectrum shows a broadening which indicates that the phosphines are not truly equivalent in the ground-state structure. The infrared spectrum of $ReH_xAlMe_2(PPh_2Me)_3$ shows two terminal absorptions characteristic of terminal Re–H bonds (i.e., above 1880 cm^{-1}) and three at lower frequencies (1803, 1765, and 1680 cm^{-1}).

The X-ray structure of $ReH_4AlMe_2(PPh_2Me)_3$, Figures 5 and 6, reveals a heavy-atom (ReP_3Al) framework composed of two nearly orthogonal planes: P3–Re–P2 and P4–Re–Al, with interplanar angle 88.4°. Two "opposite" angles among the four ligand atoms (P3–Re–P2 and P4–Re–Al) are approximately 135°, while the remaining four are in the range 93–102°. The X-ray diffraction study establishes the presence of four hydrogens bonded to rhenium, thus supporting the ^1H NMR integration. The coordination geometry about rhenium (ignoring aluminum) is satisfactorily described as pentagonal bipyramidal. Thus, the atoms H2, H3, H4, P2, and P3 form the pentagonal plane (all five atoms are within ±0.1 Å of their least-squares plane), and this plane makes an angle of 88.6° with the P4, H4, H1 plane. Atoms H1 and P4 are trans to one another (177°), and axial/equatorial angles from P4 range from 92° to 96.6°, while those from the smaller H1 range from 81° to 90°. Within the pentagonal plane (ideal angle 72°), angles range from 68° to 77°.

The key question to be answered by the structure determination is the nature of the linkage between the ReH_4P_3 pentagonal bipyramid and the $AlMe_2$ unit (i.e., the number of hydride bridges). The aluminum lies within 0.1 Å of the idealized mirror plane of the ReH_4P_3 pentagonal bipyramid (Figure 6); this is also evident in the near equality of the angles Al–Re–P (2 or 3) at 102.1° and 101.7°. Turning to the hydride positions, H4 is unequivocally terminal on Re. The remaining hydrides, H1–H3, bind not only to rhenium, but are 1.76 (5), 2.10 (8), and 1.93 (4) Å from aluminum. The longest and shortest of these Al–H distances differ by only 3.6σ (difference), so that the available data are not sufficiently precise to establish the longest distance as nonbonding to aluminum. In view of the pattern of angles within the pentagonal plane shown below (**6**), we are inclined to

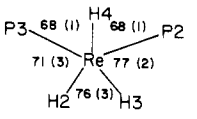

6

the idea that H2 is erroneously placed by the X-ray data in the

pentagonal plane too close to P3 and too far from H3. An H–Os–H angle of 68° is found by neutron diffraction in the pentagonal plane of $OsH_4(PMe_2Ph)_3$,[9] and would obviously lead to an H2–Al distance more compatible with bonding than the value refined here using X-ray data (2.10 (8) Å).[10]

Our preference for a tris μ-H linkage binding Re to Al in $ReH_4AlMe_2(PMePh_2)_3$ is based upon the following additional observations:

(a) The heavy atom (ReP_3Al) skeleton of the molecule has idealized mirror symmetry. On the basis of these most accurately determined atom positions, supplemented by the *assumption* that the hydride positions also obey such symmetry, Al must in fact be equidistant from H2 and H3.

(b) The bisector of the angle C6–A1–C7 does not point between H1 and H3 (as it would if H2 were terminal and the aluminate ligand were tetrahedral η^2-H_2AlMe_2), but is significantly displaced toward Re (and thus H2); see this line drawn in Figure 5. This distortion away from a tetrahedral H_2AlMe_2 unit is evident in the angles C7–A1–H (1 or 3), at 104 and 107°, compared to C6–A1–H (1 or 3), at 122 and 132°.

(c) The demand on the part of aluminum for a maximum number (i.e., 3) of hydride neighbors is evident in the geometry adopted by the ReP_3 skeleton. Consider that $ReH_4AlMe_2(PMePh_2)_3$ is merely the adduct $ReH_4P_3^-$ with $AlMe_2^+$; this is a reasonable representation if there is no Al–Re interaction *and* a η^2-$H_2AlMe_2^-$ description were to be accurate. Knowing the structure of $OsH_4(PMe_2Ph)_3$,[9] isoelectronic with $ReH_4P_3^-$, we would predict $ReH_2(\eta^2\text{-}H_2AlMe_2)(PMePh_2)_3$ to have a structure (7) in which the two most sterically accessible hydrides were employed:

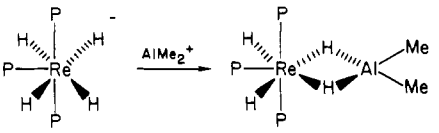

7

This *incorrect* predicted heavy atom skeleton argues for the reality of a third hydride bridge, and thus a $ReH(\eta^3\text{-}H_3AlMe_2)(PMePh_2)_3$ formulation.

Other Lewis Acids. Numerous experiments were carried out attempting dinuclear elimination between $ReH_5(PMe_2Ph)_3$ and either $HAl(i\text{-}Bu)_2$ or $HAlMe_2$. In the latter case, $ReH_4AlMe_2(PMe_2Ph)_3$ was produced but only as a component of a mixture with another trisphosphine rhenium hydride (by ^1H NMR). We attribute this to competitive elimination of CH_4 and H_2, the former giving a species like $ReH_4AlHMe(PMe_2Ph)_3$. Similar complexity was encountered with $HAl(i\text{-}Bu)_2$.

Mechanism. The compounds synthesized here are produced by a formal dinuclear alkane elimination. The rate of the reaction shows a marked dependence on the reagent rhenium hydride. Significantly, the faster reactions occur with the d^0 complexes $ReH_7(PR_3)_2$ than with the d^2 rhenium pentahydrides. Aluminum Lewis acid attack on d-electron pairs as well as single electron transfer to aluminum are therefore suggested to be mechanistically irrelevant to these dinuclear eliminations. A reaction mechanism inititated by binding of $AlMe_3$ (from the attacking reagent Al_2Me_6) to a single hydride ligand is consistent with the available observations. The slower rate with $ReH_5(PR_3)_3$ may result from steric effects in reaction with Al_2Me_6.

We have sought to observe the μ-hydride adduct proposed above between ReH_5P_3 and $AlMe_3$. Titration of increasing equivalents of Al_2Me_6 into a toluene solution of $ReH_5(PMePh_2)_3$ results in a continuous change in ^{31}P chemical shift from a value of 6.18 ppm for $ReH_5(PMePh_2)_3$ to a limiting value of 2.76 ppm when 10–15 equiv of Al/Re have been added. We take this as evidence for the equilibrium in eq 3, rapid on the ^{31}P NMR time scale (40.5

$$ReH_5(PMePh_2)_3 + {}^1/_2Al_2Me_6 \rightleftharpoons ReH_5(PMePh_2)_3AlMe_3 \quad (3)$$

MHz, 30 °C), with only a moderate equilibrium constant. The modest influence of adduct formation on ^{31}P chemical shift is reflected in the ^1H NMR; the hydride resonance of $ReH_5(PMePh_2)_3$ undergoes less than a 0.2 ppm shift in the presence of 12 equiv of added Al_2Me_6. Attempts to grow crystals of the adduct by vapor diffusion from hexane/Al_2Me_6 into a toluene/Al_2Me_6 solution of the adduct gave only crystals of $ReH_5(PMePh_2)_3$; the adduct is thus more soluble than $ReH_5(PMePh_2)_3$.

Discussion

The results presented here show that alkyl aluminum Lewis acids react cleanly with phosphino polyhydride complexes; there is no competing reaction in which the acid abstracts phosphine to form $Me_3Al{\cdot}PR_3$. To the extent that the aluminum in the product may be represented as the aluminate anions $H_{n+1}AlMe_2^{n-}$, both methane eliminations are formally two-electron reductions at rhenium ($Re^{(VII)} \rightarrow Re^{(V)}$, and $Re^{(V)} \rightarrow Re^{(III)}$). Although a steric argument has been cited above for the comparative rates of dinuclear elimination of ReH_7P_2 (faster) and ReH_5P_3 (slower), it may be that the heptavalent species is simply inherently more prone to reduction.

Although $AlPh_3$ forms an adduct with $CpFe(CO)_2^-$[11] (and AlR_3 with $CpRh(PR'_3)_2$[12]) all by direct M→Al bonding, the dinuclear eliminations reported here appear to proceed through an intermediate with Al coordinated to H. Such single hydride bridging has been claimed in $Cp_2TaH_3{\cdot}AlEt_3$[13] and has been shown crystallographically in $HAl_2Me_6^-$[14] and $Cp_3ZrHAlEt_3$.[15]

It is noteworthy that, in contrast to alanes themselves, whose H–Al proton NMR resonances are invariably broadened beyond detection,[16-18] the compounds reported here show hydride resonances of unexceptional line width and correct integrated intensity. This lack of ^{27}Al quadrupolar broadening is probably associated with the fact that these molecules are fluxional. Indeed, facile exchange of hydrides terminal on a transition metal with hydrides bridging to aluminum are without precedent.[19] It is noteworthy, in this connection, that the intramolecular exchange-averaged J_{P-H} values in the aluminum/rhenium complexes are only 2–5 Hz smaller than they are in the terminal hydrides of their precursors, ReH_7P_2 and ReH_5P_3. The mechanism of a portion of the nuclear site-exchange follows readily from the structure. Movement of the $AlMe_2$ group to nearby but nonbridged hydrogens in ReH_6AlMe_2P will average four hydrides, the two phosphorus nuclei, the inequivalent P–Me groups, and the Al*Me* groups; this motion is primarily $AlMe_2$ pivoting and hydride bending. Averaging of the remote hydrogens in $ReH_6AlMe_2P_2$ and $ReH_4AlMe_2P_3$ (as well as phosphine permutation in the latter compound) requires wholesale deformation of the coordination polyhedron about rhenium. The low-temperature ^1H and ^{31}P NMR data for $ReH_4AlMe_2(PMePh_2)_3$ show that this latter process has a higher activation energy than does pivoting of $AlMe_2$ among the three bridging hydrides in this compound. Dissociative processes (e.g., phosphine or $HAlMe_2$) play no part, since the

(9) Hart, D. W.; Bau, R.; Koetzel, T. F. *J. Am. Chem. Soc.* **1977**, *99*, 7557.

(10) Note that the thermal parameter and esd's associated with H2 are larger than those of the other hydrides.

(11) Burlitch, J. M.; Leonowicz, M. E.; Petersen, R. B.; Hughes, R. E. *Inorg. Chem.* **1979**, *18*, 1097.

(12) Mayer, J. M.; Calabrese, J. C. *Organometallics* **1984**, *3*, 1292.

(13) Tebbe, F. N. *J. Am. Chem. Soc.* **1973**, *95*, 5412.

(14) Atwood, J. L.; Hrneir, D. C.; Rogers, R. D.; Howard, J. A. K. *J. Am. Chem. Soc.* **1981**, *103*, 6787.

(15) Kopf, J.; Vollmer, H.-J.; Kaminsky, W. *Cryst. Struct. Commun.* **1980**, *9*, 985.

(16) Labinger, J. *Adv. Chem. Ser.* **1978**, *No. 167*, 149.

(17) Ouzounis, K.; Riffel, H.; Hess, H.; Kohler, V.; Weidlein, J. *Z. Anorg. Allg. Chem.* **1983**, *504*, 67.

(18) Two recent reports of detection of broad terminal Al–H resonances have appeared: (a) Girolami, G. S.; Wilkinson, G.; Thornton-Pett, M.; Hursthouse, M. B. *J. Am. Chem. Soc.* **1983**, *105*, 6752. (b) Lemkuhl, H.; Mehler, K.; Benn, R.; Rufinska, A.; Schroth, G.; Krüger, C. *Chem. Ber.* **1984**, *117*, 389.

(19) Several rigid complexes are reported in ref 18 and the following: Wailes, P. C.; Weigold, H.; Bell, A. P. *J. Organomet. Chem.* **1972**, *43*, C29.

Table V. Bond Distances (Å) and Angles (deg) for $ReH_4AlMe_2(PMePh_2)_3$

Re-P(2)	2.382 (1)
Re-P(3)	2.358 (1)
Re-P(4)	2.360 (1)
Re-Al	2.501 (2)
Re-H(1)	1.73 (5)
Re-H(2)	1.53 (8)
Re-H(3)	1.54 (4)
Re-H(4)	1.58 (3)
Al-H(1)	1.76 (5)
Al-H(3)	1.93 (4)
Al-H(2)	2.10 (8)
P(2)-C(8)	1.826 (4)
P(2)-C(9)	1.846 (4)
P(2)-C(15)	1.841 (4)
P(3)-C(21)	1.826 (4)
P(3)-C(22)	1.844 (4)
P(3)-C(28)	1.843 (4)
P(4)-C(34)	1.834 (4)
P(4)-C(35)	1.853 (4)
P(4)-C(41)	1.866 (4)
Al-C(6)	1.970 (4)
Al-C(7)	1.974 (4)
P(2)-Re-P(3)	135.5 (0)
P(2)-Re-P(4)	92.9 (0)
P(2)-Re-Al	102.1 (0)
P(3)-Re-P(4)	96.6 (0)
P(3)-Re-Al	101.7 (0)
P(4)-Re-Al	134.3 (0)
P(2)-Re-H(1)	90 (1)
P(2)-Re-H(2)	152 (3)
P(2)-Re-H(3)	77 (2)
P(2)-Re-H(4)	68 (1)
P(3)-Re-H(1)	81 (1)
P(3)-Re-H(2)	71 (3)
P(3)-Re-H(3)	145 (1)
P(3)-Re-H(4)	68 (1)
P(4)-Re-H(1)	177 (1)
P(4)-Re-H(2)	92 (3)
P(4)-Re-H(3)	93 (2)
P(4)-Re-H(4)	92 (1)
Al-Re-H(1)	45 (2)
Al-Re-H(2)	57 (3)
Al-Re-H(3)	50 (1)
Al-Re-H(4)	134 (1)
H(1)-Re-H(2)	86 (3)
H(1)-Re-H(3)	88 (2)
H(1)-Re-H(4)	89 (2)
H(2)-Re-H(3)	76 (3)
H(2)-Re-H(4)	139 (3)
H(3)-Re-H(4)	145 (2)
Re-H(1)-Al	91 (2)
Re-H(3)-Al	92 (2)
C(6)-Al-H(1)	122 (1)
C(6)-Al-H(3)	132 (1)
C(7)-Al-H(1)	104 (1)
C(7)-Al-H(3)	107 (1)
H(1)-Al-H(3)	76 (2)
Re-Al-C(6)	123.7 (1)
Re-Al-C(7)	126.3 (1)
C(6)-Al-C(7)	109.7 (2)

220-MHz ^1H NMR spectrum of $ReH_4AlMe_2(PMePh_2)_3$ in C_6D_6 shows a hydride quartet up to 120 °C.

We have concluded that $ReH_4AlMe_2(PMePh_2)_3$ contains three hydride bridges, and thus five-coordinate aluminum. There is certainly precedent for higher coordinate aluminum, especially when (small) hydride ligands are involved. These range from AlH_6^{3-} (in M_3AlH_6[20]) and $Al(\eta^2\text{-}BH_4)_3$[21] through $MeAl(\eta^2\text{-}BH_4)_2$,[22] $[(\eta^3\text{-}C_5Me_5)AlMe(\mu\text{-}Cl)]_2$,[23] $[Cp(C_5H_4)MoH]_2Al_3Me_5$,[24] $[Cp_2YCl\cdot AlH_3\cdot NEt_3]_2$,[25] $[Cp_2YCl]_2\cdot AlH_3\cdot OEt_2$,[26] and $[Ta(H_2Al(OR)_2)(dmpe)_2]_2$.[27] We have reported[28] that $Cp_2WH_2(AlMe_3)$ is not simply a Lewis acid/base adduct, but involves two bridging hydrides and higher coordinate aluminum. Finally, it has been reported[18a] recently that $Mn(AlH_4)(dmpe)_2$ is monomeric in solution but condenses to dimers in the solid via hydride bridging between five-coordinate aluminum.

In the final analysis, however, it would be prudent to consider that $ReH_4AlMe_2(PMePh_2)_3$ may contain (in H2) a hydride semibridge. The long and checkered history of L_nMHSiR_3 units, centering on whether they contain independent H and SiR_3 ligands, $M\text{-}(\mu\text{-}H)\text{-}SiR_3$ triangles, or something in between warrants careful reading,[29] particularly in view of the proximity of Si and Al in the periodic table.

Formal dissection of these bimetallic species into $ReH_4P_3^-$ or $ReH_6P_2^-$ and $AlMe_2^+$ opens the question of the particular hydrides sought out by the $AlMe_2^+$ electrophile. In the former case, pentagonal-bipyramidal $ReH_4P_3^-$ (**8**) there is obvious steric reason

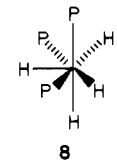

8

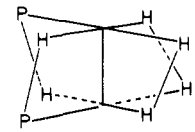

9

for choosing the face with three hydrides since this is remote from the three phosphines. We have reported[30] earlier that $Re_2H_4(PMe_2Ph)_4[P(OCH_2)_3CEt]_2$ and $Re_2H_5(PMe_2Ph)_4[P(OCH_2)_3CEt]_2^+$ each have pentagonal-bipyramidal rhenium bridging through three hydrides, one axial and two equatorial. This pattern thus appears general. In contrast, $ReH_6P_2^-$ (**9**) presents a situation of greater complexity in that there are numerous pairs of cisoid hydrides, as well as four triplets of cisoid hydrides, available for attachment of $AlMe_2^+$. Since the pair of hydrides chosen are those most remote from the two phosphine ligands, it appears that steric factors at least play a role in the outcome. A space-filling model reveals that Al*Me*/P*Me* repulsions would result from attachment of $AlMe_2$ tetrahedrally to H2 and H3. More generally, the B-sites of a dodecahedron are less sterically encumbered, as has been noted above.

Finally, the goal of maintaining an unsaturated aluminum center in the presence of reactive (i.e., catalytically useful) ligands against intra- or intermolecular ligand bridging would appear to be difficult, based on the work reported and reviewed here. Even a relatively reluctant bridge such as alkyl can bridge from a transition metal or actinide to aluminum. It would appear that the bimetallic compounds reported here will provide a new sort of bimetallic activation of entering substrate (Un) only if a hydride bridge can readily swing open with the approach of substrate (eq 4). The fluxionality of all bimetallic species reported here is cause

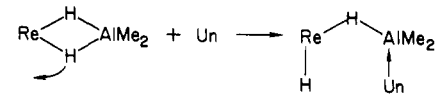

(4)

for optimism in this regard. Fugure work will explore this idea.

(20) Wiberg, E.; Amberger, E. "Hydrides of the Elements of the Main Groups I-IV"; Elsevier: Amsterdam, 1971.
(21) Almenningen, A.; Gundersen, G.; Haaland, A. *Acta Chem. Scand.* **1968**, *22*, 328.
(22) Barlow, M. T.; Dain, C. J.; Downs, A. J.; Thomas, P. D. P.; Rankin, D. W. H. *J. Chem. Soc., Dalton Trans.* **1980**, 1374.
(23) Schonberg, P. R.; Paine, R. T.; Campana, C. F. *J. Am. Chem. Soc.* **1979**, *101*, 7726.
(24) Rettig, S. J.; Storr, A.; Thomas, B. S.; Trotter, J. *Acta Crystallogr., Sect. B* **1974**, *B30*, 666. Froder, R. A.; Prout, K. *Acta Crystallogr. Sect. B* **1974**, *B30*, 2312.
(25) Lobkovsky, E. B.; Soloveychik, G. L.; Bulychev, B. M.; Erofeev, A. B.; Gusev, A. I.; Kirillova, N. I. *J. Organomet. Chem.* **1983**, *254*, 167.
(26) Lobkovsky, E. B.; Soloveichik, G. L.; Erofeev, A. B.; Bulychev, B. M.; Belskii, V. K. *J. Organomet. Chem.* **1982**, *235*, 151.
(27) McNeese, T. J.; Wreford, S. S.; Foxman, B. M. *J. Chem. Soc., Chem. Commun.* **1978**, 500.
(28) Bruno, J. W.; Huffman, J. C.; Caulton, K. G. *J. Am. Chem. Soc.* **1984**, *106*, 444.
(29) Schubert, U.; Ackermann, K.; Kraft, G.; Wörle, B. *Z. Naturforsch. B* **1983**, *38B*, 1488 and references therein.
(30) Green, M. A.; Huffman, J. C.; Caulton, K. G. *J. Am. Chem. Soc.* **1982**, *104*, 2319.

Acknowledgment. This work was supported by a grant from Dow Chemical Co. and by the M. H. Wrubel Computer Center. Cleveland Refractory Metals and Ethyl Corporation are thanked for material support. The high-field NMR spectrometer was purchased under NSF Grant No. CHE 81-05004.

Supplementary Material Available: Anisotropic thermal parameters, hydrogen positional and thermal parameters, and observed and calculated structure factors for $ReH_4AlMe_2(PPh_2Me)_3$ and $ReH_6AlMe_2(PPh_2Me)_2$ (66 pages). Ordering information is given on any current masthead page.

Reactions of the Tris(3,4,7,8-tetramethylphenanthroline)iron(II,III) Redox Couple in Nitrous Acid

M. S. Ram and David M. Stanbury*

Contribution from the Department of Chemistry, Rice University, Houston, Texas 77251.
Received June 6, 1984

Abstract: The kinetics and mechanisms of the redox reactions of $[Fe(TMP)_3]^{2+/3+}$ (TMP = 3,4,7,8-tetramethylphenanthroline) with nitrous acid have been investigated in aqueous solution at 25.0 °C in sulfate media. With a large excess of nitrite, $[Fe(TMP)_3]^{3+}$ at pH >2 is reduced quantitatively to $[Fe(TMP)_3]^{2+}$ with non-pseudo-first-order kinetics; the reaction is strongly inhibited by $[Fe(TMP)_3]^{2+}$. Acid also inhibits the reaction, but there is a direct dependence on $[NO_2^-]$. The proposed mechanism involves protonation of NO_2^- to form unreactive HNO_2; NO_2^- is oxidized quasi-reversibly by $[Fe(TMP)_3]^{3+}$ to form NO_2 with a rate constant, k_1, of 3.9×10^3 M^{-1} s^{-1}, and then NO_2 disproportionates to form NO_3^- and NO_2^-. At pH ≤ 1 $[Fe(TMP)_3]^{2+}$ is quantitatively oxidized in nitrous acid with pseudo-first-order kinetics; the reaction is strongly inhibited by NO. In the presence of added NO the rate law shows one term first order in $[HNO_2]$ and another term approximately second order in $[HNO_2]$. The path first order in $[HNO_2]$, which is undetectably slow in the absence of added NO, has a rate constant of 95 M^{-1} s^{-1}, and it is interpreted as the direct reduction of HNO_2. The path second order in $[HNO_2]$ is inverse in [NO], and it is interpreted as the rapid equilibrium formation of NO_2 and NO by disproportionation of HNO_2, followed by rate limiting ($k_{-1} = 2.0 \times 10^6$ M^{-1} s^{-1}) reduction of NO_2 by $[Fe(TMP)_3]^{2+}$. This last step is the microscopic reverse of the rate-limiting step for the reaction of NO_2^- with $[Fe(TMP)_3]^{3+}$. The equivalence of the ratio k_1/k_{-1} and the thermochemically determined equilibrium constant confirms the mechanistic assignments. The combined effects of reversible reduction of HNO_2 to NO and irreversible oxidation of HNO_2 to NO_3^- lead to biphasic kinetics in the pH range 1-2.

The chemistry of reactions with nitrous acid is broad and complex.[1-3] Aqueous solutions of nitrous acid contain a variety of minor components, many of which can be reactive. Third-order rate laws have often been reported for reactions which are first order in substrate, acidity, and N(III); such reactions are thought to proceed by a two-step mechanism in which protonation of HNO_2 yields NO^+ and then NO^+ reacts with the substrate in the rate-limiting step.[1] In several cases these NO^+ pathways have been reported for single electron oxidations of substitution inert coordination complexes;[4,5] for reactions such as these the product should be NO. Thus the rate-limiting step may involve the NO/NO^+ couple in an outer-sphere electron-transfer reaction.

Our continuing interest in the kinetics of outer-sphere redox reactions has recently embraced the notion that nuclear tunneling may be a rather significant factor, particularly for the NO_2/NO_2^- couple.[6] This is due to the high frequency of the vibrational modes that are coupled with electron transfer. The high frequencies for NO and NO^+ suggest that nuclear tunneling could be especially prominent in NO^+ pathways. The O_2/O_2^- couple is in many ways analogous with the NO/NO^+ couple. The proposal that the O_2/O_2^- couple behaves consistently with Marcus-Hush theory[7] has recently been questioned.[8] In an attempt to investigate these ideas, a study of the reactions of $IrCl_6^{3-}$ in nitrous acid was undertaken. The reaction presented unexpected difficulties, and so we were forced to reassess the body of results published on similar systems.

Particularly intriguing was a recent report[9] on the reaction of $[Fe(TMP)_3]^{2+/3+}$ (TMP = 3,4,7,8-tetramethylphenanthroline) in nitrous acid; biphasic kinetics for the reaction of $[Fe(TMP)_3]^{2+}$ were reported, and for the first phase paths were found first order in $[NO_2^-]$ and first order in $[HNO_2]$, but no NO^+ path was found. The reactions were performed in chloride-containing media; the possibility that the unusual results were due to reactivity of NOCl encouraged us to reinvestigate the reaction in chloride-free media. In the course of these studies, the reaction was found to be unexpectedly sensitive to the presence of nitric oxide. This observation entailed an extensive reinvestigation of the system. The rate law differs substantially from the prior report, but there is still no evidence for a NO^+ pathway. It is now questionable whether such a pathway has actually been observed for any outer-sphere reactions.

Experimental Section

Materials. $Li_2SO_4 \cdot H_2O$ was prepared by neutralizing Li_2CO_3 (Baker) with an appropriate amount of concentrated H_2SO_4 (MCB). The salt was recrystallized from warm water twice such that its solutions gave neutral pH.[10] $Na_4P_2O_7 \cdot 10H_2O$ (Baker) was recrystallized from warm water.[10] This buffer was used in the pH range 4-6; orthophosphate was found to be unsuitable as a buffer due to the insolubility of its lithium salt. $LiNO_3$ was prepared by neutralizing Li_2CO_3 with concentrated HNO_3 and it was recrystallized from hot water.[10] Its solutions were

(1) Ridd, J. H. *Adv. Phys. Org. Chem.* **1978**, *16*, 1.
(2) Stedman, G. *Adv. Inorg. Chem. Radiochem.* **1979**, *22*, 143.
(3) Beck, M. T.; Dozsa, L.; Szilassy, I. *J. Ind. Chem. Soc.* **1974**, *51*, 6.
(4) Bates, J. C.; Reveco, P.; Stedman, G. *J. Chem. Soc., Dalton Trans.* **1980**, 1487.
(5) Reveco, P.; Stedman, G. *Z. Anal. Chem.* **1979**, *295*, 252.
(6) Stanbury, D. M.; Lednicky, L. A. *J. Am. Chem. Soc.* **1984**, *106*, 2847.
(7) (a) Stanbury, D. M.; Haas, O.; Taube, H. *Inorg. Chem.* **1980**, *19*, 518. (b) Stanbury, D. M.; Mulac, W.; Sullivan, J. C.; Taube, H. *Inorg. Chem.* **1980**, *19*, 3735. (c) Stanbury, D. M.; Gaswick, D.; Brown, G. M.; Taube, H. *Inorg. Chem.* **1983**, *22*, 1975.
(8) McDowell, M. S.; Espenson, J. H.; Bakac, A. *Inorg. Chem.* **1984**, *23*, 2232.
(9) Epstein, I. R.; Kustin, K.; Simoyi, R. H. *J. Am. Chem. Soc.* **1982**, *104*, 712.
(10) Perrin, D. D.; Armarego, W. L. F.; Perrin, D. R. "Purification of Laboratory Chemicals", 2nd ed.; Pergamon Press: New York, 1980; pp 499, 500, and 533.

0002-7863/84/1506-8136$01.50/0